

**U.S. Department of Energy
FreedomCAR and Vehicle Technologies, EE-2G
1000 Independence Avenue, S.W.
Washington, D.C. 20585-0121**

FY 2007

**REPORT ON TOYOTA/PRIUS MOTOR TORQUE
CAPABILITY, TORQUE PROPERTY, NO-LOAD BACK-EMF,
AND MECHANICAL LOSSES – REVISED MAY 2007**

Prepared by:

Oak Ridge National Laboratory

Mitch Olszewski, Program Manager

Submitted to:

Energy Efficiency and Renewable Energy
FreedomCAR and Vehicle Technologies
Vehicle Systems Team

Susan A. Rogers, Technology Development Manager

May 2007

Engineering Science and Technology Division

**REPORT ON TOYOTA/PRIUS MOTOR
TORQUE CAPABILITY, TORQUE
PROPERTY, NO-LOAD BACK EMF, AND
MECHANICAL LOSSES**

J. S. Hsu, Ph.D.

C. W. Ayers

C. L. Coomer

R. H. Wiles

T. A. Burress

Oak Ridge National Laboratory

S. L. Campbell

K. T. Lowe

R. T. Michelhaugh

Oak Ridge Institute for Science and Education

Publication Date(s): Original Report–September 30, 2004

First Revision–July 2005

Second Revision–May 2007

Prepared by the
OAK RIDGE NATIONAL LABORATORY
Oak Ridge, Tennessee 37831
managed by
UT-BATTELLE, LLC

for the
U.S. DEPARTMENT OF ENERGY
Under contract DE-AC05-00OR22725



DOCUMENT AVAILABILITY

Reports produced after January 1, 1996, are generally available free via the U.S. Department of Energy (DOE) Information Bridge:

Web site: <http://www.osti.gov/bridge>

Reports produced before January 1, 1996, may be purchased by members of the public from the following source:

National Technical Information Service

5285 Port Royal Road

Springfield, VA 22161

Telephone: 703-605-6000 (1-800-553-6847)

TDD: 703-487-4639

Fax: 703-605-6900

E-mail: info@ntis.fedworld.gov

Web site: <http://www.ntis.gov/support/ordernowabout.htm>

Reports are available to DOE employees, DOE contractors, Energy Technology Data Exchange (ETDE) representatives, and International Nuclear Information System (INIS) representatives from the following source:

Office of Scientific and Technical Information

P.O. Box 62

Oak Ridge, TN 37831

Telephone: 865-576-8401

Fax: 865-576-5728

E-mail: reports@osti.gov

Web site: <http://www.osti.gov/contact.html>

This report was prepared as an account of work sponsored by an agency of the United States Government. Neither the United States Government nor any agency thereof, nor any of their employees, makes any warranty, express or implied, or assumes any legal liability or responsibility for the accuracy, completeness, or usefulness of any information, apparatus, product, or process disclosed, or represents that its use would not infringe privately owned rights. Reference herein to any specific commercial product, process, or service by trade name, trademark, manufacturer, or otherwise, does not necessarily constitute or imply its endorsement, recommendation, or favoring by the United States Government or any agency thereof. The views and opinions of authors expressed herein do not necessarily state or reflect those of the United States Government or any agency thereof.

CONTENTS

| | Page |
|---|-------------|
| LIST OF FIGURES | iii |
| LIST OF TABLES | iii |
| REVISIONS (MAY 2007)..... | iv |
| PUBLISHED TORQUE CAPABILITY OF THE TOYOTA/PRIUS MOTOR..... | 1 |
| TORQUE PROPERTY OF PM RELUCTANCE MOTOR | 2 |
| TEST SETUP | 3 |
| POWER SUPPLY FOR CONDUCTING MOTOR TORQUE CAPBILITY TEST AT ZERO SPEED..... | 6 |
| MEASURED TORQUE OF TOYOTA/PRIUS 2004 MOTOR | 7 |
| MOTOR TORQUE-PROPERTY ANALYSES | 8 |
| MEASURED BACK-EMF | 10 |
| CONCLUSIONS..... | 12 |
| APPENDIX: PROCEDURS FOR MEASURING NO-LOAD LOSSES ON TOYOTA/PRIUS MOTOR | 14 |
| I. TEST SETUP | 14 |
| II. TESTS | 15 |
| II.a Prius Hybrid Drive No-Load Loss | 16 |
| II.b No-Load Loss Excluding Motor Rotor | 16 |
| II.c No-Load Loss Excluding Motor Rotor and Planetary Gears | 16 |

LIST OF FIGURES

| Figure | Page |
|---|------|
| 1 Comparison of output power and torque vs. speed between the 2003 (THS) and 2004 (THSII) Prius motors | 1 |
| 2 Phasor diagrams and symbol definitions of a PM reluctance motor..... | 2 |
| 3 Motor, generator, and engine of the 2004 Toyota/Prius hybrid THS II system..... | 4 |
| 4 Test setup | 5 |
| 5 Load torque adjustment mechanism during torque test | 5 |
| 6 Pointer is attached to non-driving side shaft of motor | 6 |
| 7 Three-phase current phasors and their instantaneous current values | 7 |
| 8 Circuit diagram for motor torque-capability test | 7 |
| 9 Motor torque vs. electrical angle of Prius motor at various currents (revised configuration)..... | 8 |
| 10 Motor peak torque values vs. the motor current amplitude (revised configuration)..... | 8 |
| 11 Tested torque of motor divided into synchronous and reluctance torques (revised configuration)..... | 9 |
| 12 Prius 2004 rotor punchings | 10 |
| 13 Measured back-emfs vs. speed | 11 |
| 14 Back-emfs of the Prius motors..... | 11 |
| 15 The gear and motor mechanical losses | 12 |
| I.1 Motor, generator, engine, differential gear assembly, and axles of the Toyota/Prius hybrid traction drive system..... | 14 |
| I.2 Wheel axle 1 of Toyota/Prius motor is coupled to a dynamometer driven by an adjustable-speed motor | 15 |
| I.3 Transmission differential gear assembly..... | 15 |
| I.4 “Dummy” rotor assembly | 16 |
| I.5 Planetary gear assembly..... | 17 |
| I.6 Toyota/Prius hybrid-drive transmission assembly | 17 |

LIST OF TABLES

| Table | Page |
|--|------|
| 1 Power and torque of the permanent magnet (PM) synchronous motor of Toyota/Prius hybrid THS and THSII systems | 1 |

REVISIONS (MAY 2007)

Revisions are in red and have been made to Figs. 4–6, 9–11, Fig. 13, and Fig. I.2. Revisions have also been made to the text on page 5 and in item #6, Conclusions, on page 12. Revisions authored by T. A. Burrell.

In today's hybrid vehicle market, the Toyota/Prius drive system is currently considered the leader in electrical, mechanical, and manufacturing innovations. It is significant that in today's marketplace, Toyota is able to manufacture and sell the vehicle for a profit.

This project's objective is to test the torque capability of the 2004 Prius motor and to analyze the torque properties relating to the rotor structure. The tested values of no-load back electromotive force (emf) and mechanical losses are also presented.

PUBLISHED TORQUE CAPABILITY OF THE TOYOTA/PRIUS MOTOR

In today's hybrid vehicle market, the Toyota/Prius motor has one of the highest-power-density traction motors.

Figure 1 shows the published comparison of the output power and torque vs. speed between the 2003 (THS) model and 2004 (THSII) model of the Prius motors. Both the output power and the torque of the motor are significantly increased in the new model.

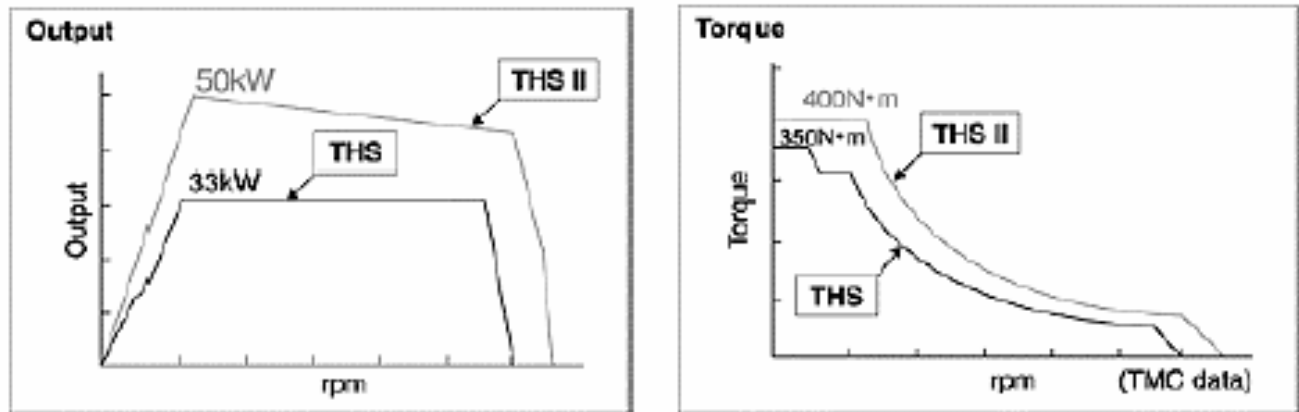


Fig. 1. Comparison of output power and torque vs. speed between the 2003 (THS) and 2004 (THSII) Prius motors.

Source: *Development of Hybrid Electric Drive System Using a Boost Converter*, Masaki Okamura, Eiji Sato, and Shoichi Sasaki, Toyota Motor Corporation.

The power at base speed as tabulated in Table 1 is 50 kW. This is significantly higher than the 33 kW of the older model. The torque of 400 Nm is also higher than the 350/305 Nm of the previous year's model.

Table 1. Power and torque of the permanent magnet (PM) synchronous motor of Toyota/Prius hybrid THS and THSII systems

| | Model (2004) | Model (2003) |
|---------|------------------|-----------------------|
| Power: | 50 kW | 33 kW |
| | at base speed | 1040–5600 rpm |
| Torque: | 400 Nm | 350Nm 305 Nm |
| | up to base speed | 0–400 rpm 400–1000rpm |

In Toyota's publications, the authors have not found the distinctions between the continuous rating and the peak-power rating. Temperature-rise tests will be conducted to find out the continuous rating and the permissible time for the peak rating.

TORQUE PROPERTY OF PM RELUCTANCE MOTOR

Figure 2 is a phasor diagram of the phase variables of a PM reluctance machine. The phase voltage is symbol V ; phase current, I ; phase back-emf, E ; direct-axis, suffix d (d-axis); quadrature-axis, suffix q (q-axis); and load angle, δ . The assumptions of sinusoidal time and space variables are used in the phasor diagram of Fig. 2. The three-phase power, P , going into the motor is derived through the products of the voltage projections and the currents.

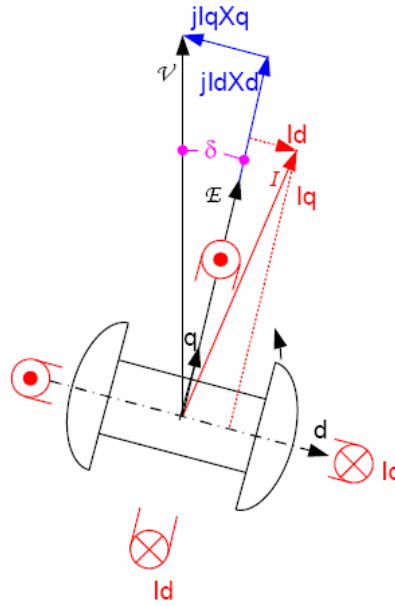


Fig. 2. Phasor diagrams and symbol definitions of a PM reluctance motor.

$$P = 3 (V \cos\delta I_q - V \sin\delta I_d). \quad (1)$$

The $V \cos\delta$ and the $V \sin\delta$ terms of Eq. (1) can be rewritten according to Fig. 2. This gives

$$P = 3 [(E + I_d X_d) I_q - I_q X_q I_d]. \quad (2)$$

Substituting $I_d = (V \cos\delta - E)/X_d$, and $I_q = (V \sin\delta)/X_q$ into Eq. (2) gives

$$P = 3 [VE \sin\delta / X_d + 0.5V^2 \sin 2\delta (1/X_q - 1/X_d)]. \quad (3)$$

The first term inside the brackets of Eq. (3) represents the synchronous power corresponding to the PMs that is proportional to $\sin\delta$. The second term is a typical reluctance power that varies according to $\sin 2\delta$ and results from the difference of the reciprocals of the quadrature-axis and direct-axis reactances.

One of the design goals of the Toyota/Prius motor is to increase the difference between the q-axis and the d-axis reactances, yet retain a sufficiently high synchronous PM power.

The motor shaft output power is the product of the motor torque and the angular frequency of the shaft rotation. At zero speed, regardless of how high the torque is, the shaft output power is zero, because the angular frequency of the shaft is zero.

The torque of a PM reluctance motor, such as the Prius motor, is developed through the interaction between the armature current and the flux produced by the PMs and the reluctance paths. At zero speed, although the shaft output power is zero, the power of the PMs and the difference between the q- and d-axis inductances are already established. These power derivations can be applied to the PM and reluctance torques that are proportional to the $\sin\delta$ and the $\sin 2\delta$, respectively. For the same reason, the motor torque capability obtained at zero speed serves as a good indicator of the motor behavior throughout the motor's speed range.

The torque capability of the motor measured at zero speed is relatively simple to obtain. This is accomplished by separating the tested torque into its fundamental and second harmonic components. The fundamental component will indicate the PM torque component, and the second-order harmonic will represent the additional reluctance torque produced by the reluctance difference.

TEST SETUP

Figure 3 shows the assembly of the Toyota/Prius hybrid THSII drive train system.

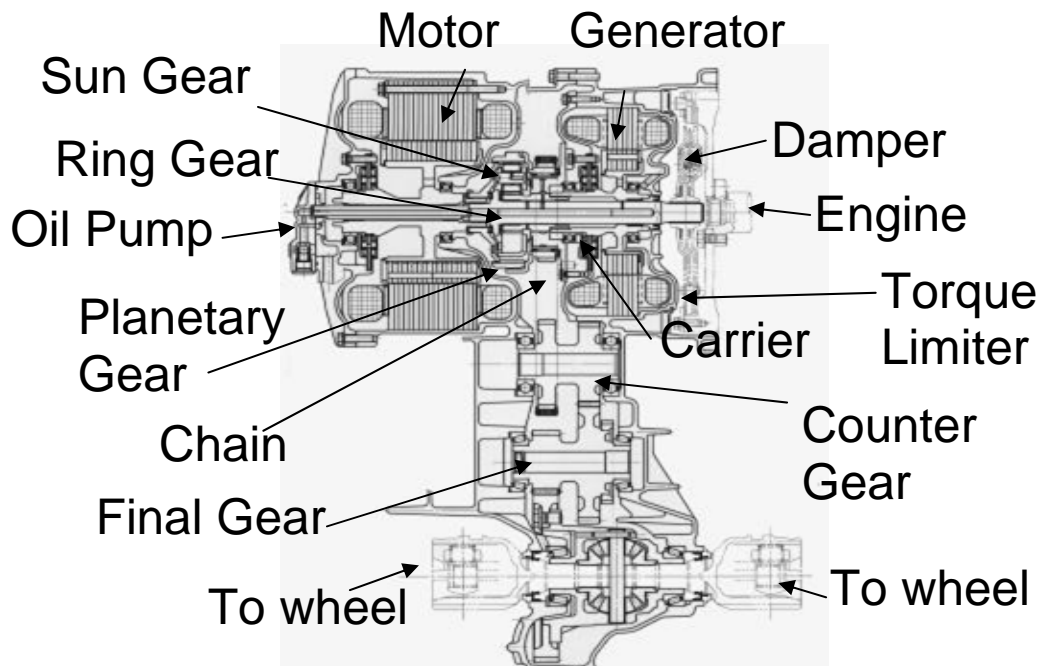


Fig. 3. Motor, generator, and engine of the 2004 Toyota/Prius hybrid THSII system.

Source: *Development of Electric Motors for the TOYOTA Hybrid Vehicle "PRIUS,"* Kazuaki Shingo, Kaoru Kubo, Toshiaki Katsu, and Yuji Hata, Toyota Motor Corporation.

As shown in Fig. 3, the motor of the Toyota/Prius is not a stand-alone motor. The motor shaft is coupled to a set of gears and then to the wheel shafts without a direct motor-torque shaft coming out from the frame. The non-driving side motor shaft is not strong enough for loading but can be coupled for the rotor position indication. In initial tests, the driveshaft was modified and connected to the test setup. Because the two wheel axle shafts are the outputs of a differential gear set driven by the motor, the locked torque of the motor can be measured through a torque gauge at one of the two wheel shafts when the other wheel shaft is locked. The torque ratio from the motor shaft to the wheel is determined by the revolution ratio between the wheel shaft and the motor shaft. For the Toyota/Prius hybrid THS II drive train system being tested, the torque at the wheel axle shaft multiplied by 0.486 gives the motor torque.

A revised test setup method to access the motor shaft was implemented to obtain a more accurate representation of the motor torque. The motor shaft is connected directly to ring of the planetary gear, and the engine spline is connected to the sun of the planetary gear. Therefore, if the planetary carriers are forced to be stationary, the direct motor torque appears unchanged at the engine spline, which is externally accessible. Thus the planetary carriers were welded and more accurate torque and position data was produced.

Figure 4 shows the initial test setup. Starting from the left side of the figure, one side of the torque gauge is coupled to a load adjustment arm. The angular position of the arm can be adjusted by a jack bolted to the end of the arm. The other side of the torque gauge is coupled to one of the two wheel axial shafts coming out from the motor and drive-train housing.

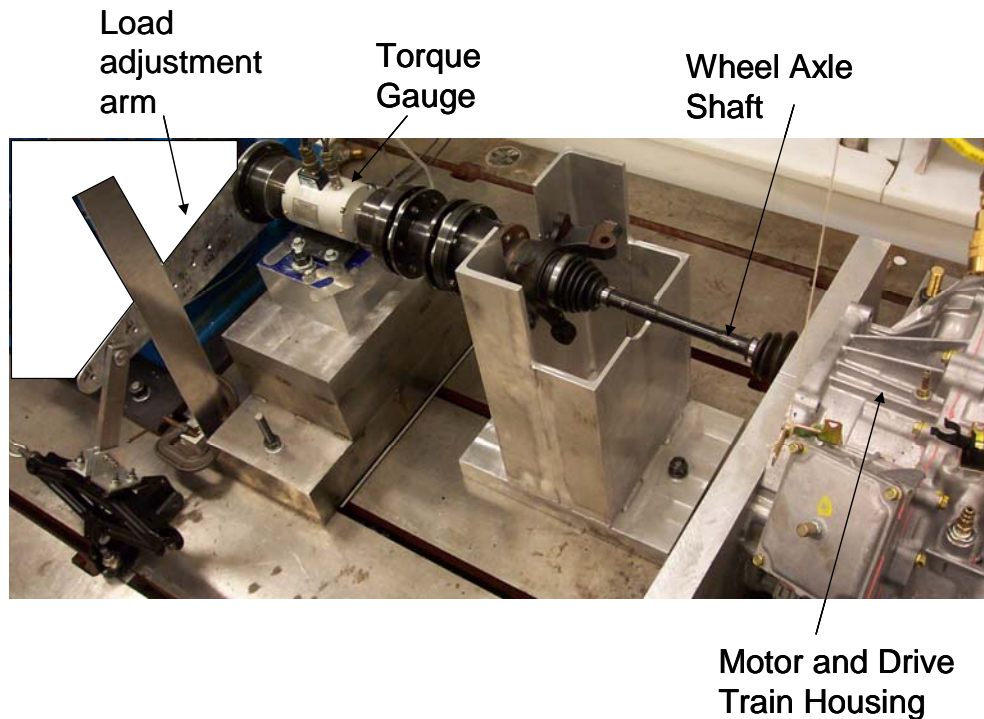


Fig. 4. Test setup (initial configuration).

The load adjustment arm and the coarse angle indicators viewed from the end of the torque gauge are shown in Fig. 5. The coarse rotor angle indicators can only be used as a reference for the coarse adjustment of the rotor position because the wheel axle shaft has a significant twist under a high torque. The direction of the jack's controlled movements are also indicated in the figure.

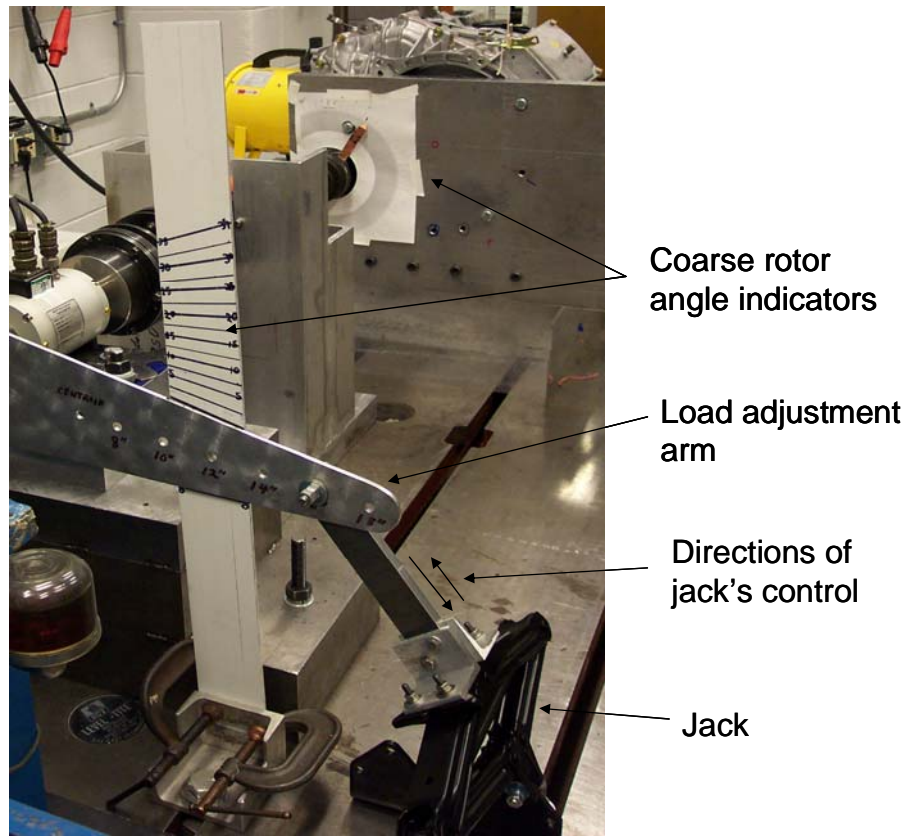


Fig. 5. Load torque adjustment mechanism during torque test (initial configuration).

Please note that the locked rotor torque data presented in this report was not produced using the setup described in the preceding paragraphs. A revised test setup method to access the motor shaft was implemented to obtain the more accurate data presented in this report.

Figure 6 illustrates the setup viewed from the end of the motor and drive train housing. The second wheel axle shaft is mechanically locked. A pointer is attached to the motor shaft's non-drive side. The rotor angular displacement can be accurately obtained from this setup. The zero position refers to the position without any load torque.

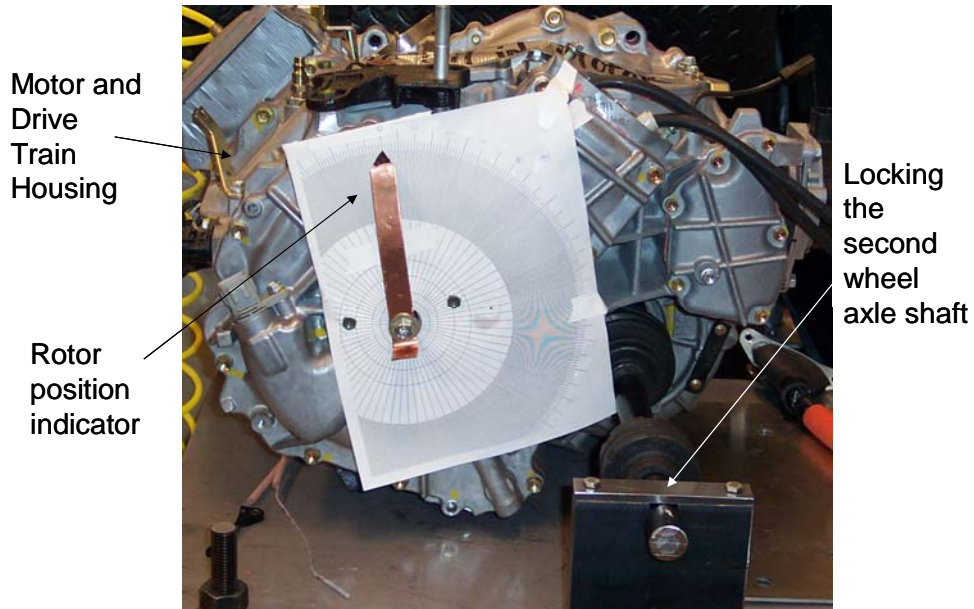


Fig. 6. Pointer is attached to non-driving side shaft of motor (initial configuration).

POWER SUPPLY FOR CONDUCTING MOTOR TORQUE CAPABILITY TEST AT ZERO SPEED

Unlike in an induction motor that requires a rotating stator field to produce a rotor current, the power of the PMs and the reluctance difference between the direct and quadrature axes of the Prius motor are established without relying on the rotating stator field. Figure 7 shows a snapshot of the three-phase current phasors rotating at the synchronous speed for this motor torque capability test. Their projections to the vertical coordinate represent their instantaneous current values.

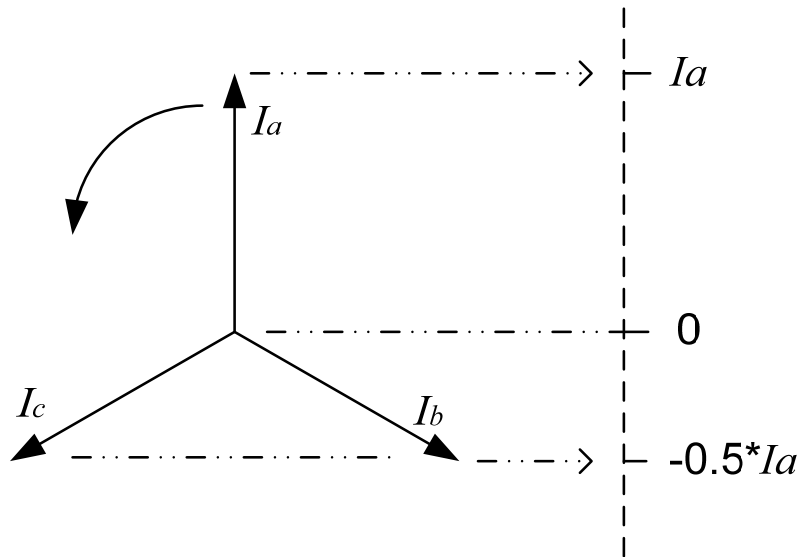


Fig. 7. Three-phase current phasors and their instantaneous current values.

The instantaneous values at the instance shown in Fig. 7 are I_a for phase a, $-0.5*I_a$ for phase b, and $-0.5*I_a$ for phase c. These values will be used for the stator armature currents throughout the test.

A dc power supply can be used to supply the needed currents for the three phases, as shown in the circuit diagram of Fig. 8. The phase-a current would be divided into two halves that go through the phase b and c windings in an opposite direction from the phase-a current direction.

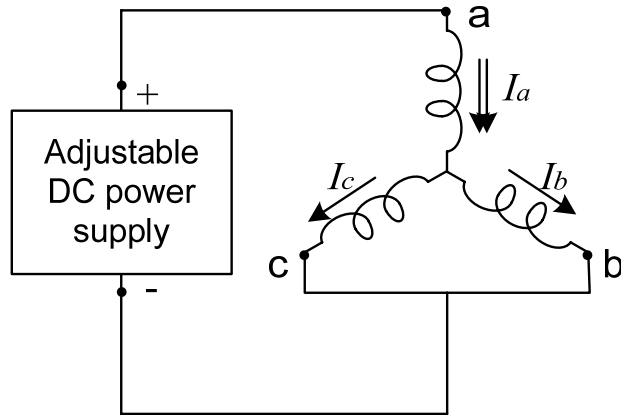


Fig. 8. Circuit diagram for motor torque-capability test.

MEASURED TORQUE OF TOYOTA/PRIUS 2004 MOTOR

Figure 9 shows the motor torque vs. the rotor electrical angle away from the no-torque (or zero angle) position tested at 50, 75, 100, 125, 150, 200, and 250 A, respectively. The motor is an eight-pole motor; therefore, the electrical angle is four times the mechanical angle. A current amplitude of 250 A produces about 340 Nm, and it is estimated that about 325 A is required to generate 400 Nm of torque. To ensure no winding damage or magnet demagnetization was incurred prior to additional benchmarking tests, the current was limited to 250 A.

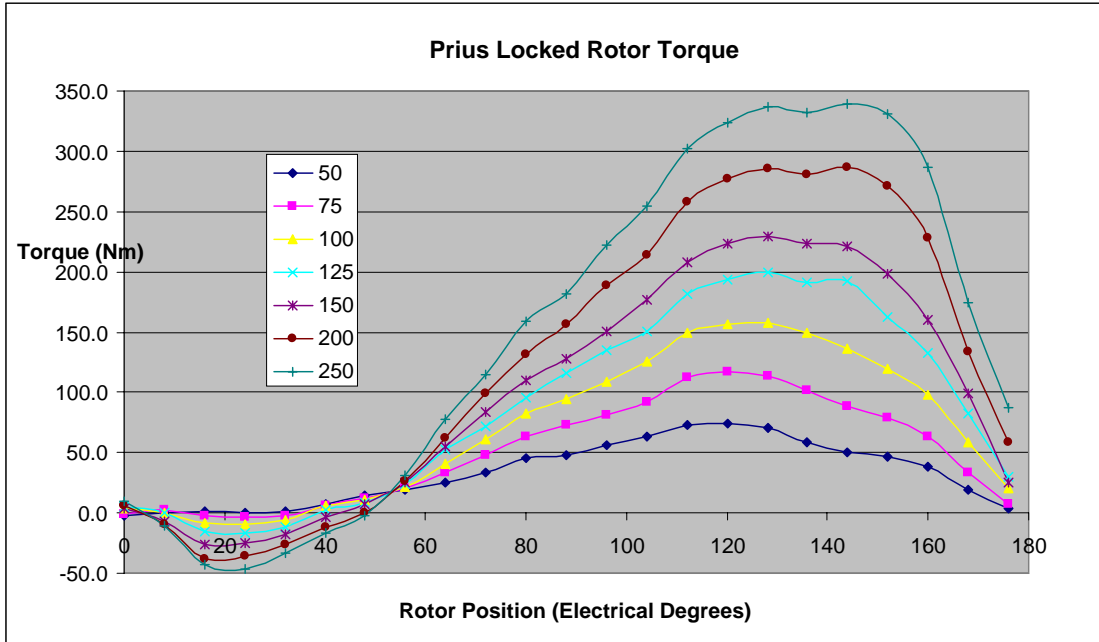


Fig. 9. Motor torque vs. electrical angle of Prius motor at various currents (revised configuration).

MOTOR TORQUE-PROPERTY ANALYSES

The peak torque values vs. current magnitudes are plotted in Fig. 10. A saturation of torque production gradually takes place as the current increases above about 125 A. The effects of saturation are especially significant above current amplitudes of 150 A.

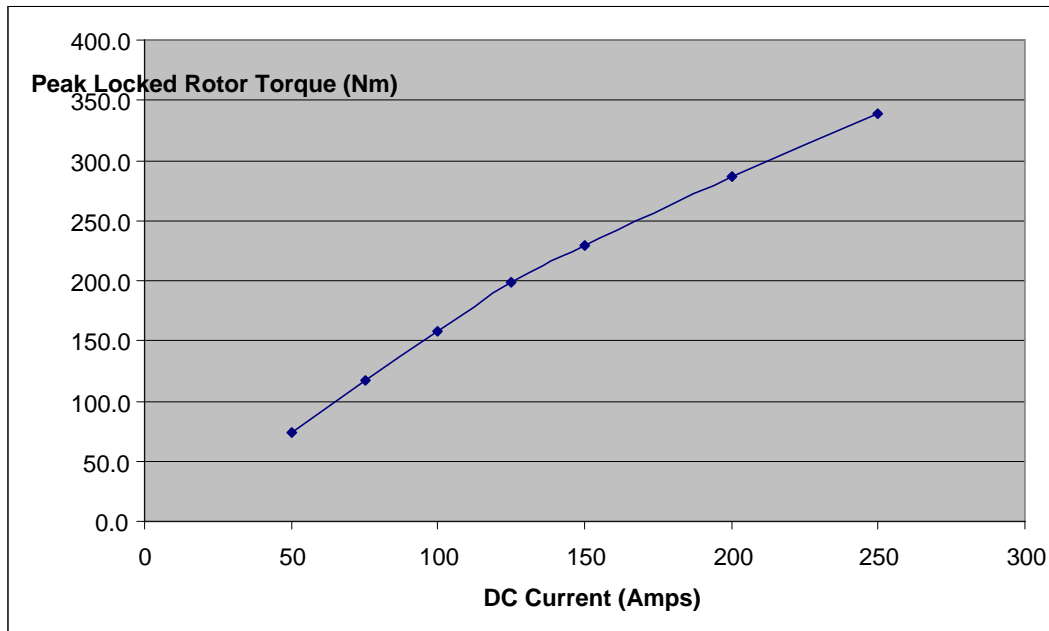


Fig. 10. Motor peak torque values vs. the motor current amplitude (revised configuration).

As an example, Fig. 11 shows that at the phase current amplitude of 150 A, the tested motor torque can be broken down into a fundamental distribution and a second harmonic distribution. As explained, the fundamental distribution represents the synchronous PM torque, and the second harmonic distribution corresponds to the reluctance torque. In this case, the ratio of the amplitudes of the synchronous PM torque and the reluctance torque is 1.47 (176 Nm/120 Nm).

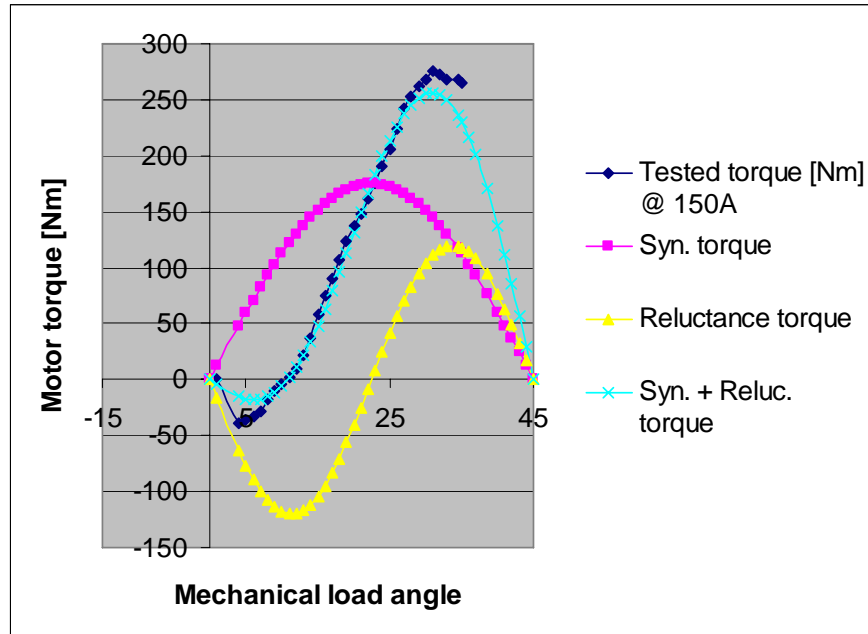


Fig. 11. Tested torque of motor divided into synchronous and reluctance torques (initial configuration).

The significant reluctance torque component is contributed by the rotor punching pattern shown in Fig. 12. It clearly shows a reluctance difference between the d- and q-axes. In this case, the q axis (i.e., located between the PM poles) allows the magnetic flux to go through easily. For this situation, when X_q is greater than X_d , the reluctance torque component vs. load angle shown in Fig. 11 begins with the negative values.

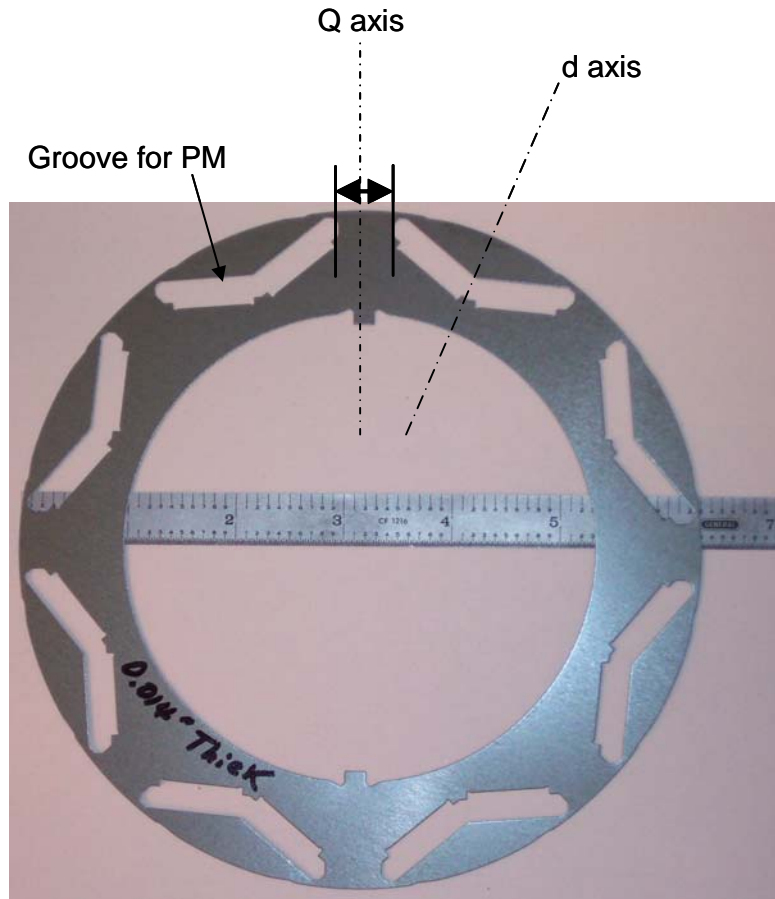


Fig. 12. Prius 2004 rotor punchings.

MEASURED BACK-EMF

The peak and rms values of the measured back emf vs. motor speed are shown in Fig. 13. The peak voltage at 6000 rpm is 850 V. Because of the voltage harmonics, the ratio of the peak value and rms value is greater than 1.414 of the conventional sinusoidal waveforms.

At 3600 rpm, the back-emf reaches 500 V. The Prius dc bus voltage can be boosted to 500 V, significantly lower than the value of 850 V obtained at 6000 rpm. This means that the Prius system has to rely on field weakening or current-angle advancement for a significant region at high speeds.

Because of the high back-emf, the insulation requirement on the motor is high. Fortunately, the Prius motor uses direct oil cooling for its winding. The oil helps to increase the insulation strength.

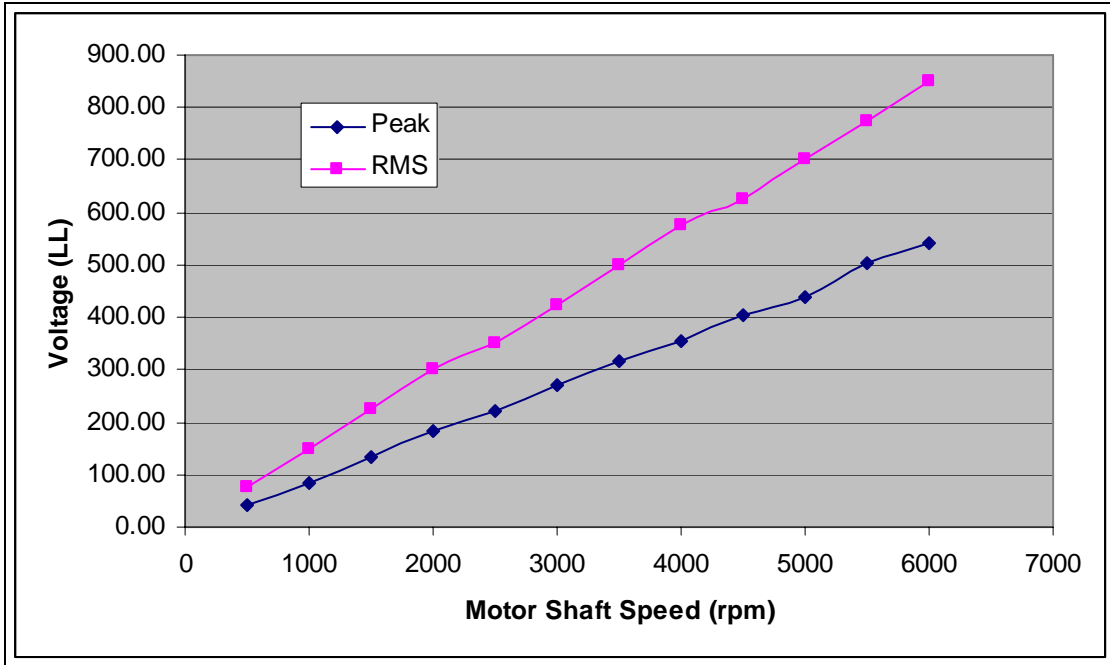


Fig. 13. Measured back-emfs vs. speed.

The measured back emf traces are illustrated in Fig. 14.

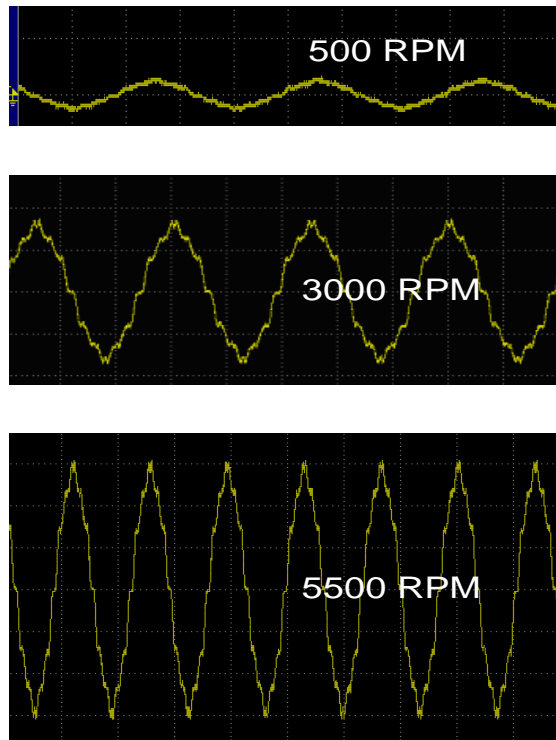


Fig. 14. Back-emfs of the Prius motor.

The tested no-load mechanical and core losses for the gears, rotor, and planetary, as well as the total losses, are plotted in Fig. 15. It is clear that the gear system produces significant losses. With a 30-kW load, the 2.4-kW mechanical losses calculate to a 7.4% (i.e., $100 \cdot 2.4 / (30 + 2.4) = 7.4\%$) efficiency drop at 6000 rpm. The no-load losses are reduced at lower speeds.

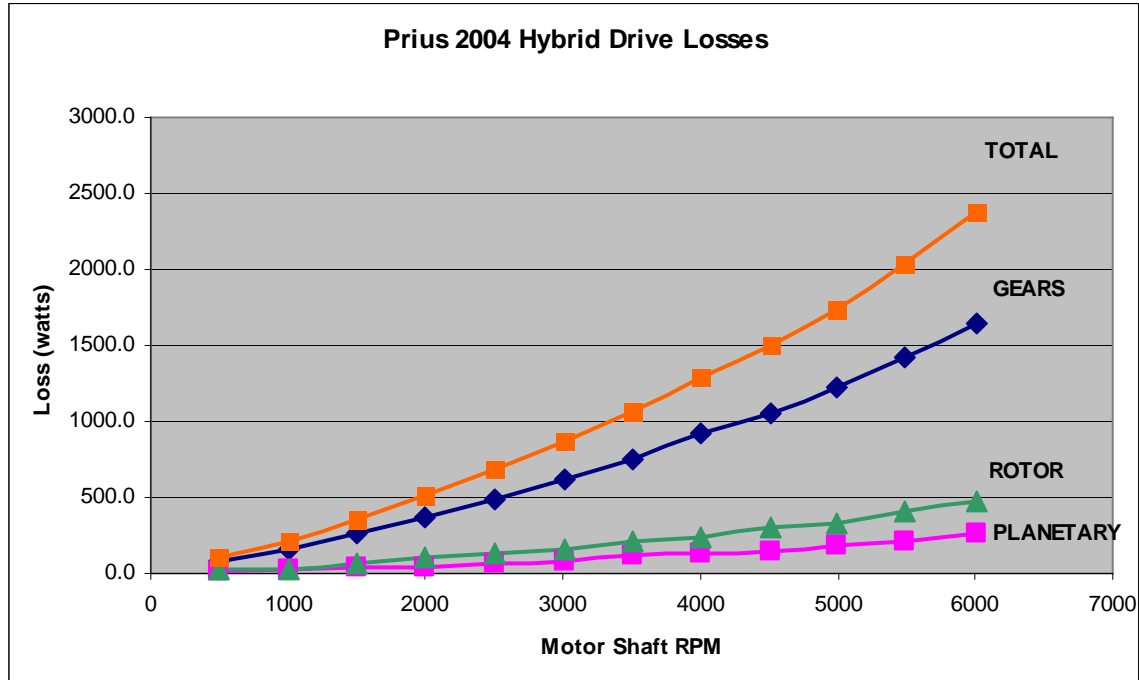


Fig. 15. The gear and motor mechanical losses.

CONCLUSIONS

1. The motor torque capability test and the torque property analysis of the Toyota/Prius 2004 motor were conducted at the Oak Ridge National Laboratory. This report can be used as a reference for the torque-capability and torque-property assessments of similar types of motors (i.e., PM, reluctance, PM/reluctance, etc.).
2. The motor torque capability is a direct indicator of the motor power density.
3. The torque of a PM reluctance motor such as the Prius motor is developed through the interaction between the armature current and the flux produced by the PMs and the reluctance paths. At zero speed, although the shaft output power is zero, the PMs and the difference between the quadrature- and direct-axis inductances are already established. The motor torque capability obtained at zero speed serves as a good indicator of the motor's behavior throughout the motor's speed range.
4. The torque of the 2004 Prius motor can be separated into PM and reluctance torques that are proportional to the $\sin\delta$ and the $\sin 2\delta$, respectively.
5. The torque vs. motor load angle is measured directly by welding the planetary gears.
6. The Prius motor meets the 400-Nm torque mentioned in Toyota's publication at zero speed. **The current amplitude required to reach the torque is about 325 A.** The reluctance torque component is very significant. For the amplitude of the 150 A case, the ratio of the amplitudes of the synchronous PM torque component and the reluctance torque component is 1.47 (176 Nm/120 Nm).
7. The design of the rotor punching plays an important role in the torque production.

8. The back emf of the motor is quite high. At 3600 rpm, the back emf reaches 500 V; at 6000 rpm, it reaches 850 V. This means that in order to run the motor, the Prius system has to advance the current angle for a significant region at high speed.
9. Because of the high back emf, the insulation requirement for the motor is high. Fortunately, the Prius motor uses direct oil-droplet cooling for its windings. The oil helps to increase the insulation strength.
10. The gear system is a source of mechanical losses. At 6000 rpm, with a 30-kW load, the total mechanical loss (excluding the electromagnetic losses) of the motor and its gears is 7.4%. The mechanical loss decreases at lower speed.

APPENDIX

PROCEDURES FOR MEASURING NO-LOAD LOSSES ON TOYOTA/PRIUS MOTOR

This section gives a detailed explanation of the tests performed to obtain Fig. 15 in this report.

I. TEST SETUP

Figure I.1 shows the motor, generator, engine, differential gear assembly, and axles of the Toyota/Prius hybrid traction drive system.

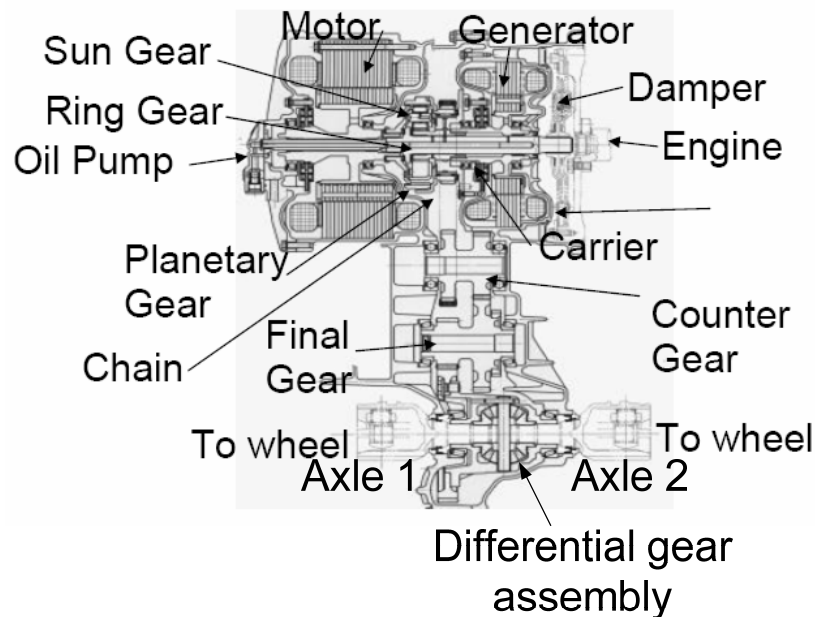


Fig. I.1. Motor, generator, engine, differential gear assembly, and axles of the Toyota/Prius hybrid traction drive system.

Figure I.2 shows that the *wheel axle 1* of the Prius drive system was directly coupled in line with the dynamometer driven by an adjustable-speed motor to drive the Toyota traction motor. The torque gauge that measures the energy going into the motor is located between *axle 1* and the dynamometer. The loss measurements are calculated from the torque gauge and rotation speed readings. The product of torque in Newton-Meter times the angular frequency of the rotation gives the power going into the motor.

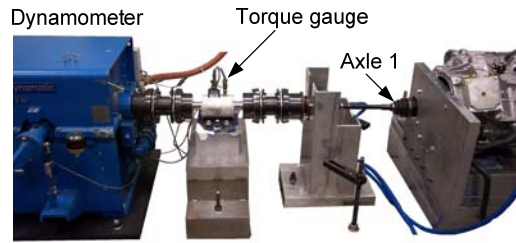


Fig. I.2. Wheel axle 1 of Toyota/Prius motor is coupled to a dynamometer driven by an adjustable-speed motor (initial configuration).

Since the differential gear in the transmission will spin when the wheels are rotating at different rates, the differential gears were welded together to transmit power to the motor. This changed the axle to motor speed ratio from 2.057:1 to 4.114:1.

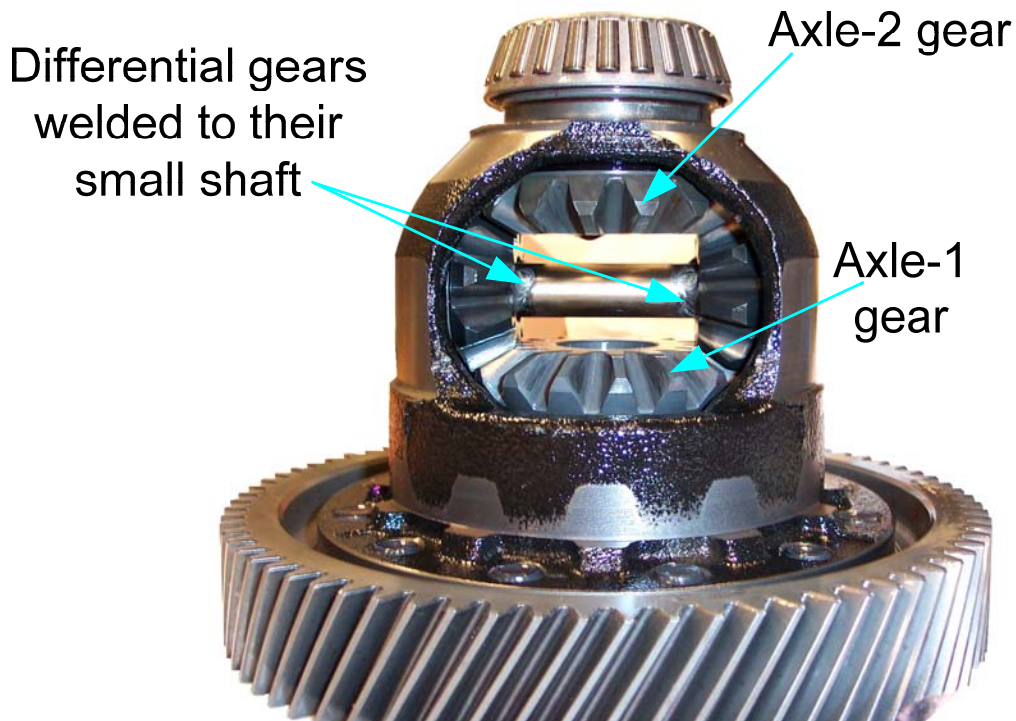


Fig. I.3. Transmission differential gear assembly.

II. TESTS

Two of the three motor phases were connected to a Yokogawa PZ-4000 power meter for measuring RMS, PP voltage, and electrical motor frequency. Several tests were run to ensure that heat build-up did not affect the measurements. Once the data was compiled for the entire motor, segments of the transmission and motor were removed to quantify the losses sustained by the planetary gears, the rotor, and the transmission drive gears.

II.a Prius Hybrid Drive No-Load Loss

The total Prius hybrid drive no-load loss is obtained by running the Prius drive as shown in Fig. I.2. The product of torque in Newton-Meter times the angular frequency of the rotation gives the total no-load loss of the Prius drive.

II.b No-Load Loss Excluding Motor Rotor

Next, the motor rotor was removed and replaced with a “dummy” rotor as shown in Fig. I.4; this rotor contained no laminations or PMs. The tests were rerun in this configuration which determined the losses due to the transmission drive train (motor no-load core loss) = (total loss) – (loss without rotor).

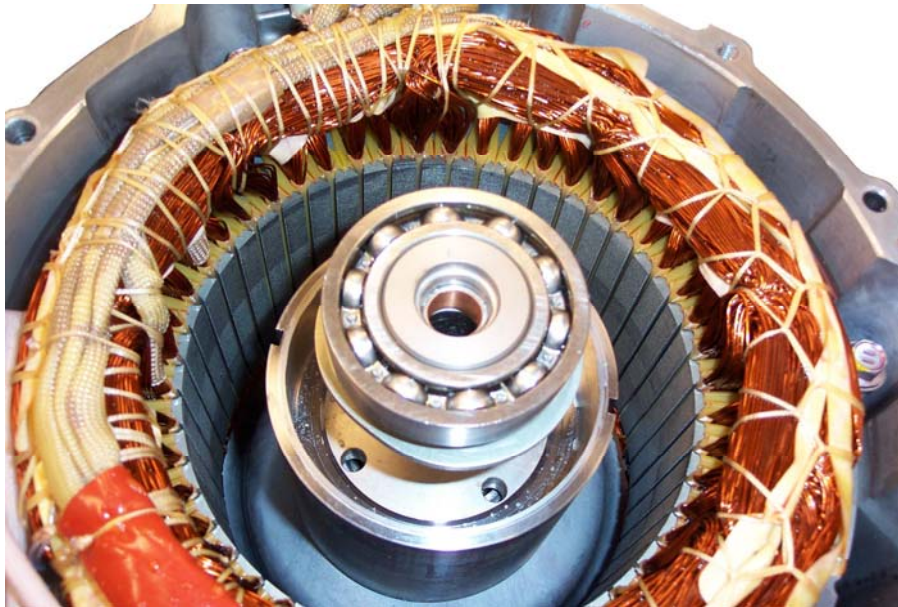


Fig. I.4. “Dummy” rotor assembly.

II.c No-Load Loss Excluding Motor Rotor and Planetary Gears

The planetary gears shown in Fig. I.5 were removed for this test. This configuration allows for the measurement of the losses due to the gear train within the drive system (gear train loss) = (total drive loss) – (loss without motor rotor & planetary gear losses).



Fig. I.5. Planetary gear assembly.

The final test was conducted with only the main drive gears shown in Fig. I.6; drive chain, and the welded axle differential in place.



Fig. I.6. Toyota/Prius hybrid-drive transmission assembly.

The Prius 2004 hybrid drive losses vs. motor shaft speed are plotted in Fig. 15 of this report.

Once all of the above data was collected and analyzed, the Prius traction drive motor was re-assembled, with all drive line components, for the collection of data on the back-emf of the motor.

DISTRIBUTION

Internal

1. D. J. Adams
2. C. W. Ayers
3. S. Campbell
4. C. L. Coomer
5. E. C. Fox
6. J. S. Hsu
7. K. Lowe
8. L. D. Marlino
9. J. W. McKeever
10. T. Michelhaugh
11. R. H. Wiles
12. Laboratory Records

External

14. S. A. Rogers, U.S. Department of Energy, EE-2G/Forrestal Building, 1000 Independence Avenue, S.W., Washington, D.C. 20585.
15. E. J. Wall, U.S. Department of Energy, EE-2G/Forrestal Building, 1000 Independence Avenue, S.W., Washington, D.C. 20585.